Observational inferences of lateral eddy diffusivity in the halocline of the Beaufort Gyre

(submitted to Geophys. Res. Lett.)

GIANLUCA MENEGHELLO, JOHN MARSHALL,
SYLVIA T. COLE, MARY-LOUISE TIMMERMANS

Key points

- **Eddy diffusivity in the Beaufort Gyre (BG) ranges from $100 - 500\ m^2/s$ near the surface, decaying rapidly with depth across the halocline**
- **Eddy-induced upwelling largely compensates downward Ekman pumping**
- **Lateral eddy diffusivity plays a zero-order role in the freshwater budget**

Eddy diffusivity in the limit of vanishing residual mean

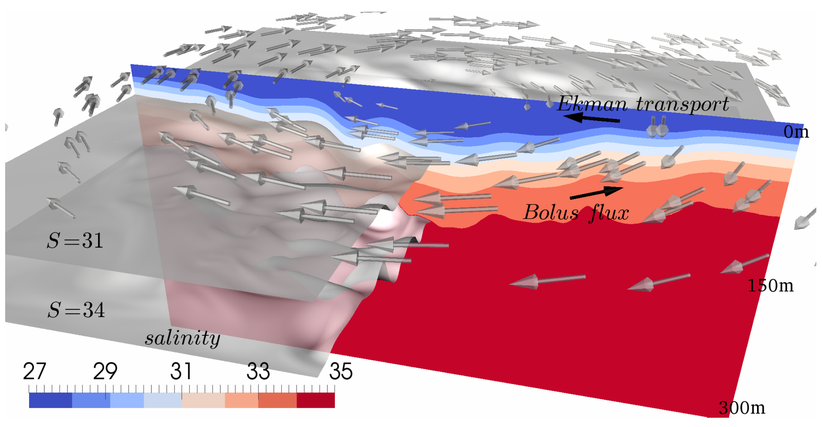

Adopting a residual mean theory framework (Andrews and McIntyre, 1976; Marshall and Radko, 2003; Plumb and Ferrari, 2005), we use observations of Ekman pumping and isopycnal slopes to infer the magnitude of the eddy diffusivities required to bring the residual circulation in the halocine of the BG to zero.

We are then considering the limit case in which bolus transport by eddies are sufficiently strong to exactly balance the Eulerian-mean flow set up by the wind:

$$\Psi_{res} = \underbrace{\overline{\Psi}}_{\frac{\overline{\tau}}{\rho_0 f_0}} + \underbrace{\Psi^*}_{\frac{\overline{v_r' b'}}{\overline{b}_z} \approx -K_D \frac{\overline{b}_r}{\overline{b}_z}} = 0.$$

where $\overline{v_r' b'}$ is the radial eddy buoyancy flux and $\overline{b}_z$ is the vertical stratification. As is conventional (Gent and Mcwilliams, 1990) we characterise the efficiency of eddy transport by an eddy diffusivity and write $\overline{v_r' b'} = -K_D \overline{b}_r$. The eddy diffusivity can then be estimated as

$$K_D = \frac{1}{\rho_0 f_0} \frac{\overline{\tau}}{\overline{s}} \quad \text{where} \quad \overline{s} = -\frac{\overline{b}_r}{\overline{b}_z} = \frac{\partial \overline{h}}{\partial r}.$$

Here h is the depth of the isopycnal, r is the radial coordinate and $\overline{s}$ the slope of the isopycnal of the time and azimuthally averaged density field. For computational convenience, rather than integrating along geopotential height contours, we use the divergence and Stokes theorems to rewrite the eddy diffusivity as

$$K_D = \frac{1}{\rho_0 f_0} \frac{\int \nabla \times \tau \, dA}{\int \nabla^2 h \, dA},$$

where the integrals are performed over the area circumscribed by a geopotential height contour and τ and h are averaged only in time.

Observations of Ekman pumping and isopycnal slopes

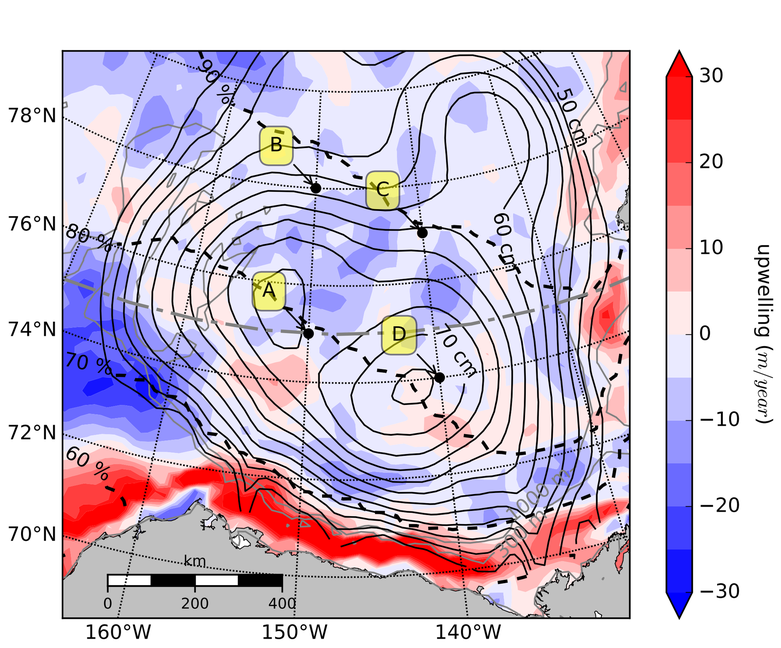

The 2003-2012 climatology of Ekman pumping w_{Ek} (color) and geopotential height D computed from the 2005-2012 World Ocean Atlas climatology (black contours). Thick dashed lines show mean ice concentration.

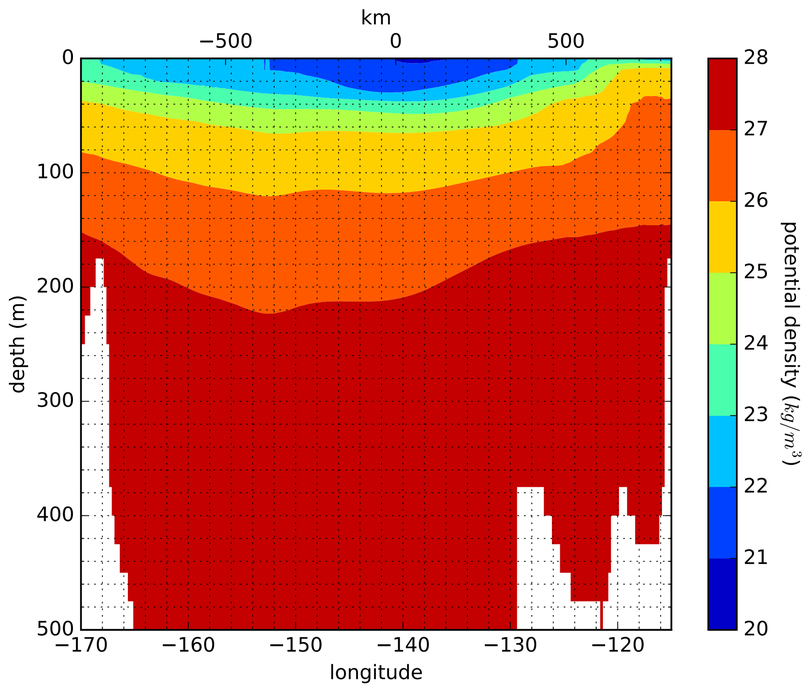

Hydrographic section of potential density (referenced to the surface) at 75°N (see gray dash-dotted line in left panel), computed from the World Ocean Atlas climatology.

Implied eddy diffusivity

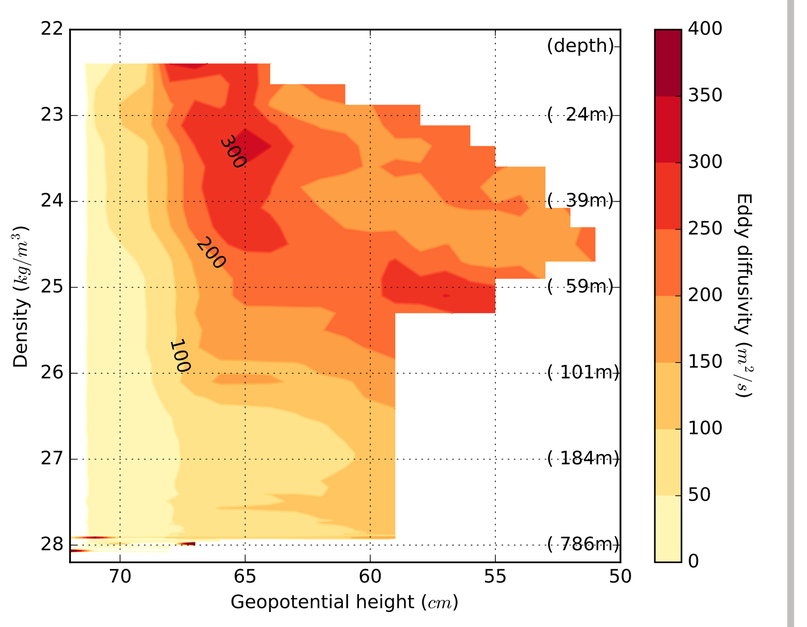

Eddy diffusivity K_D implied by the zero-residual-mean circulation hypothesis, as a function of density and geopotential height contour; the depth in parenthesis is the mean depth of the isopycnal.

Eddy diffusivity inferred from the BG moorings

We then estimate horizontal eddy diffusivity from temperature, salinity and velocity profiles obtained from four Beaufort Gyre Observing System (BGOS) moorings.

A mixing length framework is employed as described by Cole et al. (2015). The mixing length, λ, and horizontal diffusivity, K_λ, are estimated as:

$$\lambda = \frac{\overline{\theta'_{iso} \theta'_{iso}}^{1/2}}{|\nabla \overline{\theta}_{iso}|}$$

$$K_\lambda = c_0 \lambda \overline{u' u'}^{1/2},$$

where θ_{iso} is the temperature along a density surface, u the horizontal velocity vector, and c_0 a mixing efficiency (Tennekes, 1972; Armi and Stommel, 1983; Naveira Garabato et al., 2011; Abernathey and Cessi, 2014). The mixing efficiency is taken to be $c_0 = 0.16$ (Wunsch, 1999; Klocker and Abernathey, 2014). Primed quantities denote a fluctuation from the mean; temperature and velocity were first averaged with a 30-day timescale, and then all variability at timescales larger than one year was removed. The timescales are chosen to exclude higher frequency variability primarily in the velocity observations, and to represent the mesoscale dynamics of the system. Overbar denotes a temporal average over all years. The spatial gradient of the mean temperature field, $\nabla \overline{\theta}_{iso}$, is estimated along density surfaces from MIMOC (Schmidtko et al., 2013) at a $100\,\mathrm{km}$ scale. The calculation is performed independently on each density surface and for each mooring.

A range of mixing lengths, velocity fluctuations, and diffusivities were found at the four moorings. Mixing length values ranged from less than 50 to near $200\,\mathrm{km}$. Velocity fluctuations decayed by more than a factor of two between $70\,\mathrm{m}$ and $300\,\mathrm{m}$ depth, and then remained constant at approximately $0.02\,\mathrm{m\,s^{-1}}$. Both mixing length and velocity fluctuations are small in comparison to other regions (Cole et al., 2015).

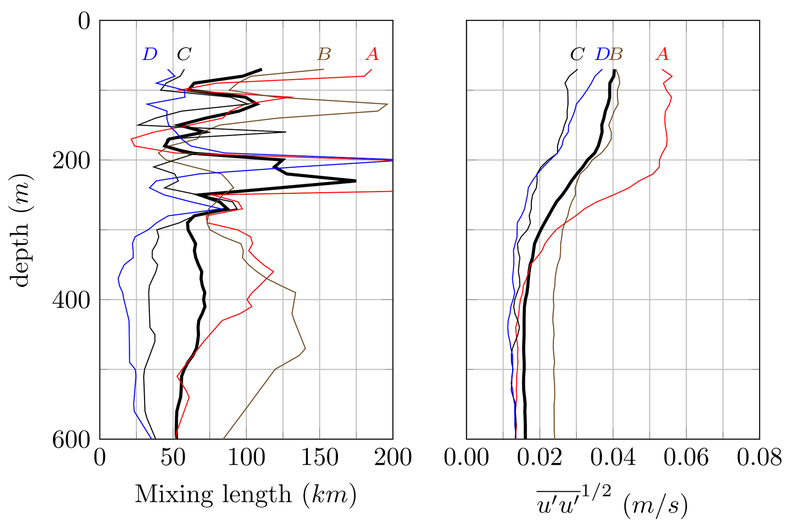

Profiles of (left) mixing length and (right) magnitude of velocity fluctuations. The black thick line denotes the mean among the four moorings.

Implied eddy diffusivity

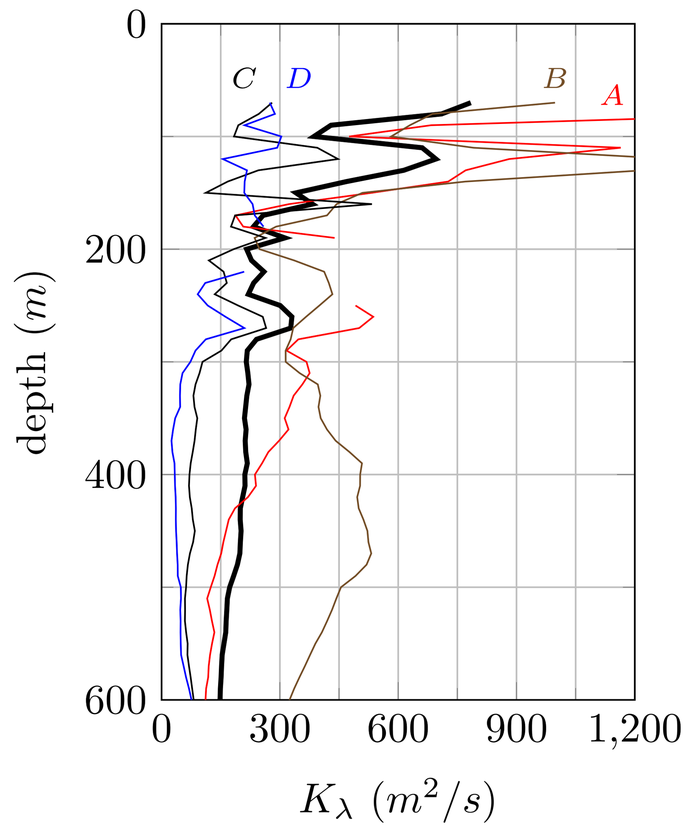

Eddy diffusivity K_λ inferred from the BG moorings, as a function of depth. Eddy diffusivities range from 100 to more than $600\,\mathrm{m^2\,s^{-1}}$, with a factor of two decay with depth from 70 to $300\,\mathrm{m}$ arising from that of the velocity fluctuations. The black thick line denotes the mean among the four moorings.

References

Abernathey, R. and Cessi, P. (2014). Topographic Enhancement of Eddy Efficiency in Baroclinic Equilibration. *Journal of Physical Oceanography*, 44(8):2107–2126.

Andrews, D. G. and McIntyre, M. E. (1976). Planetary Waves in Horizontal and Vertical Shear: The Generalized Eliassen-Palm Relation and the Mean Zonal Acceleration. *Journal of the Atmospheric Sciences*, 33:2031–2048.

Armi, L. and Stommel, H. (1983). Four Views of a Portion of the North Atlantic Subtropical Gyre. *Journal of Physical Oceanography*, 13(5):828–857.

Cole, S. T., Wortham, C., Kunze, E., and Owens, W. B. (2015). Eddy stirring and horizontal diffusivity from Argo float observations: Geographic and depth variability. *Geophysical Research Letters*, 42(10):3989–3997.

Gent, P. R. and Mcwilliams, J. C. (1990). Isopycnal Mixing in Ocean Circulation Models. *Journal of Physical Oceanography*, 20(1):150–155.

Klocker, A. and Abernathey, R. (2014). Global Patterns of Mesoscale Eddy Properties and Diffusivities. *Journal of Physical Oceanography*, 44(3):1030–1046.

Marshall, J. and Radko, T. (2003). Residual-Mean Solutions for the Antarctic Circumpolar Current and Its Associated Overturning Circulation. *Journal of Physical Oceanography*, 33(11):2341–2354.

Naveira Garabato, A. C., Ferrari, R., and Polzin, K. L. (2011). Eddy stirring in the Southern Ocean. *Journal of Geophysical Research: Oceans*, 116(9).

Plumb, R. A. and Ferrari, R. (2005). Transformed Eulerian-Mean Theory. Part I: Nonquasigeostrophic Theory for Eddies on a Zonal-Mean Flow. *Journal of Physical Oceanography*, 35(2):165–174.

Schmidtko, S., Johnson, G. C., and Lyman, J. M. (2013). MIMOC: A global monthly isopycnal upper-ocean climatology with mixed layers. *Journal of Geophysical Research: Oceans*, 118(4):1658–1672.

Tennekes, H. (1972). *A First Course in Turbulence*.

Wunsch, C. (1999). Where do ocean eddy heat fluxes matter? *Journal of Geophysical Research: Oceans*, 104(C6):13235–13249.